Behavior of the aqueous sodium chloride solution from molecular simulations and theories

Tong, Jiahuan; Peng, Baoliang; Kontogeorgis, Georgios M.; Liang, Xiaodong

Published in:
Journal of Molecular Liquids

Link to article, DOI:
10.1016/j.molliq.2022.121086

Publication date:
2023

Document Version
Publisher's PDF, also known as Version of record

Journal of Molecular Liquids 371 (2023) 121086

Contents lists available at ScienceDirect

Journal of Molecular Liquids

journal homepage: www.elsevier.com/locate/molliq

Behavior of the aqueous sodium chloride solutions from molecular simulations and theories

Jiahuan Tong [a], Baoliang Peng [b,*], Georgios M. Kontogeorgis [a], Xiaodong Liang [a,*]

[a] Center for Energy Resources Engineering, Department of Chemical and Biochemical Engineering, Technical University of Denmark, Kgs. Lyngby, 2820, Denmark
[b] Research Institute of Petroleum Exploration & Development (RIPED), PetroChina, Beijing 100083, China

ARTICLE INFO

Article history:
Received 19 August 2022
Revised 13 December 2022
Accepted 14 December 2022
Available online 19 December 2022

Keywords:
MD simulations
Molecular theories
Self-diffusion
Molar conductivity
Static relative permittivity

ABSTRACT

Molecular simulations and theories are important tools for studying electrolyte solutions. In this work, molecular dynamics simulations with one of the most widely used force field combination of water and alkali and halide monovalent ion parameters were first conducted for the aqueous sodium chloride solutions to predict density, self-diffusion coefficients and molar conductivity. Then the radial distribution functions were analyzed to obtain the first shell solvation radii and coordination numbers of ions, which were found practically unchanged against concentration. Together with the force field parameters, they were further applied into various molecular theories to predict the Gibbs energy of solvation, static relative permittivity, mean ionic activity coefficients and molar conductivity. It is remarkable to see that the mean ionic activity coefficients and molar conductivity can be predicted with deviations of 1.1 % and 1.4 %, respectively, up to 6 mol/kg H_2O.

1. Introduction

Electrolyte solutions are widely involved in many fields such as life, chemistry, environment, geology, oceanography, material sciences as well as chemical and biochemical, pharmaceutical, electrical and petroleum engineering [1–6]. There are numerous types of electrolyte solutions in the mentioned applications, while the aqueous solutions of inorganic salts are one of the most important types. Even though the dissolution of inorganic salts in water is a basic physical and chemical process, the understanding of the process and the best practice how to simulate and model these systems are still far away from clear [7–13]. Over several decades, many molecular simulations, theories and models have been devoted to the study of salt solutions, especially the aqueous solutions of sodium chloride (NaCl), because it is one of the most common substances in many applications and it has widely available experimental data [8–13].

Numerous combinations of water and ionic force field models have been proposed and applied for studying the structure and properties of the aqueous solutions of NaCl [14–27]. The combination of the Joung and Cheatham (JC) ion model and the extended simple point charge (SPC/E) water model has become one of the most popular approaches. The SPC/E model was developed by Berendsen et al. [28] and it gives a simple parameterization for the effective charges and short-range potential, that is, the water molecules are represented by three point charges in a rigid geometry with an H—O—H bond angle (109.5°) slightly different from that in the gas-phase H_2O molecule (104.5°). Although the model does not allow any polarization or dissociation of the water molecules, it accurately reproduces some of the thermodynamic and dielectric properties of water [28–32]. In particular, the SPC/E model predicts accurately the density of water at ambient condition, and it predicts the critical point of water at 362–374 °C with a density of 0.29–0.326 g/cm^3, while the critical point of real water is about 374 °C with a density of 0.322 g/cm^3. It is one of the most popular water models when studying the aqueous electrolyte solutions [8,9,13,33,34]. The parameters of the JC ion model were optimized following a self-consistent approach, with the hydration free energy as the primary target property, considering a balance of the lattice energy and interionic distances of the crystals, as well as minimizing the binding energy and binding distance of an ion with a single water molecule. The combination of SPC/E and JC force fields have been applied very successfully to numerous studies, for structures such as radial distribution function, coordination numbers (ion pairs, hydration numbers), residence times, and for properties and phenomena such as density, static relative permittivity, Gibbs energy of solvation, chemical potential, activity coefficient, solubility, nucleation, diffusion, and so on [8,13,17,25,33–42].

* Corresponding authors.
E-mail addresses: pengbl@petrochina.com.cn (B. Peng), xlia@kt.dtu.dk (X. Liang).

https://doi.org/10.1016/j.molliq.2022.121086
0167-7322/

Molecular theories have been actively used for the study of aqueous electrolyte solutions, especially the advanced equations of state and the theories involved in these models in recent years [11,12,43–66]. The Debye-Hückel theory [67] is probably the most widely used theory for the ion-ion electrostatic forces. Despite the fact that this theory was proposed and developed about 100 years ago, very active research from different angles have been carried out around this theory in recent years [68–87]. The static relative permittivity, usually also known as dielectric constant, is a very important input parameter when applying the Debye-Hückel theory. There is still no consensus, however, in the context of an electrolyte equation of state, whether the static relative permittivity of the solvent (either constant or with a very weak electrolyte concentration dependency), or that of the solution, or the thermodynamic part of the solution's permittivity shall be used in the theory. It is known that the self-potential (or solvation) term, often expressed as the Born equation [88], does not contribute to the activity coefficients (non-ideality) if the static relative permittivity is electrolyte concentration independent [12]. It has been shown in recent studies that the Debye-Hückel theory, naturally including the Born equation, can predict qualitatively correct, sometimes quantitatively satisfactory, the behavior of mean ionic activity coefficients with experimental ionic radii and static relative permittivity for many different types of salts [78,89–91]. The equation for conductivity corresponding to the extended Debye-Hückel theory has also shown a very promising prediction capability, especially for 1:1 electrolytes [92].

On one hand, molecular simulations show capabilities in estimating thermodynamic and dynamic (transport) properties directly via the molecular interaction models, as well as in linking the relationship between the microscopic structure and properties. However, molecular simulations usually take long computational time (hours, days, weeks and sometimes even longer, depending on the complexity and conditions of the system). Molecular theory-based thermodynamic models, on the other hand, can provide very fast calculations, but usually only for thermodynamic properties. In order to obtain the structural information, additional frameworks need to be included, for example classical density functional theory or density gradient theory for interfacial tension and adsorption [93–97]. Both molecular simulations and molecular models need to fit parameters to properties, and sometimes it is very challenging to maintain the predictive capability for various types of systems. The modern advanced thermodynamic models have a theoretical basis and molecular simulations have also played an important role in developing some of the most popular models [98,99].

The main purpose of this work is to present molecular dynamics simulations using the state-of-the-art force fields within the pairwise Coulombic and Lennard-Jones framework towards a doable purpose, first to show the capabilities of simulations in estimating density, self-diffusion coefficients and molar conductivity, and also to provide input parameters, solvation radii and hydration numbers of ions, to molecular theories for predicting Gibbs energy of solvation, static relative permittivity, mean ionic activity coefficient and molar conductivity of aqueous NaCl solutions. To the best of our knowledge, this might be the first practice in the category that molecular theories with direct inputs from molecular simulations can accurately predict various types of properties, when comparing with experimental data.

The paper is organized as follows. In Section 2, the methods are described, including the setup of molecular simulations and the most relevant equations of the used molecular theories. The results from molecular simulations and molecular theories are presented and discussed in two subsections in Section 3, followed by the conclusions in Section 4.

2. Methods

2.1. Molecular simulations

Using the SPC/E water model [28] and the JC ion model for Na^+ and Cl^- [17], the molecular dynamics (MD) simulations were performed using LAMMPS [100]. The initial configurations of the simulated models were constructed using Packmol [101,102] and Moltemple [103]. For every simulation system, first an isothermal-isobaric ensemble (NPT) simulation was performed for 27 ns (ns) at 298 K and 1 bar with the relaxed process using the Nose-Hoover barostat and thermostat, following an integration time step of 1 fs (fs). Then another NPT simulation was performed, with the simulation trajectory saved every 1000 simulation steps, for 24 ns to equilibrate the system and to calculate density and to analyze microstructures from the last few nanoseconds, Finally, a canonical ensemble (NVT) simulation was performed for 22 ns to calculate the self-diffusion coefficients. In all simulations, we have chosen to fix the number of water molecules to 2800 and the numbers of NaCl molecules are 25, 50, 100, 150, 200, 250 and 300, which approximately correspond to molality m equal to 0.5, 1, 2, 3, 4, 5 and 6 mol/kg H_2O, respectively, according to the following relation

$$m = \frac{n_{\mathrm{NaCl}}}{n_{\mathrm{H2O}} \times M_{\mathrm{H2O}}} \tag{1}$$

where m is the molality (mol/kg H_2O) and M_{H2O} is the molecular weight of water ($M_{\mathrm{H2O}} = 0.018015$ kg/mol), while n represents the number of molecules.

2.2. Molecular theories

It is common practice to relate the Gibbs energy of solvation with the Born equation [88,104,105]

$$\Delta G_i^s = \frac{N_A}{1000}\frac{e^2 Z_i^2}{8\pi\varepsilon_0}\frac{1}{R_i}\left(\frac{1}{\varepsilon_w} - 1\right) \tag{2}$$

where ΔG_i^s is the Gibbs energy of solvation (kJ/mol) of component i with valency (charge number) Z_i and solvation radius R_i, N_A is the Avogadro constant, e is the elementary charge, ε_0 is the vacuum permittivity, and ε_w is the static relative permittivity of water.

It has been shown in previous works [90], that the activity coefficient of ions can be obtained from the extended Debye-Hückel theory combined with the so-called self-potential term (also commonly known as the Born equation)

$$\ln\gamma_i = -\frac{e^2 Z_i^2}{8\pi k_B T\varepsilon_0\varepsilon_r}\frac{\kappa}{1+\kappa\sigma_\pm} + \frac{e^2 Z_i^2}{8\pi k_B T\varepsilon_0}\frac{1}{R_i}\left(\frac{1}{\varepsilon_r} - \frac{1}{\varepsilon_w}\right) \tag{3}$$

where γ_i is the activity coefficient of ion i, k_B is the Boltzmann constant, T is the absolute temperature, ε_r is the static relative permittivity of the solution, $\sigma_\pm$ is the distance of closest approach of two ions (often the average ion radii are used), and κ is the inverse Debye screening length, given by

$$\kappa = \frac{N_A e^2}{k_B T\varepsilon_0\varepsilon_r}\sum_j c_j Z_j^2 \tag{4}$$

where c_j is the molar concentration (mol/L) of ions.

The mean ionic activity coefficient is calculated from the activity coefficients of (individual) ions, given in Equation (3). For an 1:1 electrolyte, such as NaCl, it can be written

$$\ln\gamma_\pm = \frac{1}{2}\left[\ln\gamma_i(\mathrm{Na}^+) + \ln\gamma_i(\mathrm{Cl}^-)\right] \tag{5}$$

And it is usually the molality based mean ionic activity coefficient reported as the experimental data in literature, and they are related via

$$\ln\gamma_{\pm}^{m} = \ln\gamma_{\pm} + \ln x_w \tag{6}$$

where x_w is the mole fraction of water.

As seen from Equations (3) and (4), the static relative permittivity of the solution ε_r is needed when calculating activity coefficients of ions and the electrolyte. Maribo-Mogensen et al. developed a theory to predict the static relative permittivity of pure compounds and mixtures including electrolyte solutions, allowing a natural integration with the association theory based equations of state [106,107]. For a non-electrolyte system, it reads

$$\frac{(2\varepsilon_r+\varepsilon_\infty)(\varepsilon_r-\varepsilon_\infty)}{\varepsilon_r(\varepsilon_\infty+2)^2} = \frac{\rho}{9\varepsilon_0 k_B T}\sum_i x_i g_i \mu_{0,i}^2 \tag{7}$$

where ρ is the molar number density, x_i, g_i and $\mu_{0,i}$ are the mole fraction, Kirkwood g-factor and dipole moment of component i, and ε_∞ is the static relative permittivity at infinite frequency, obtained from the Clausius-Mossotti relation

$$\frac{\varepsilon_\infty-1}{\varepsilon_\infty+2} = \frac{\rho}{3\varepsilon_0}\sum_i x_i \alpha_{0,i} \tag{8}$$

where $\alpha_{0,i}$ is the molecular polarizability of species i.

The Kirkwood g-factor is given by the following equation

$$g_i = 1 + \sum_j \frac{N_{ij}P_{ij}\cos\left(\gamma_{ij}\right)}{P_i\cos(\theta_{ij})+1}\frac{\mu_{0,j}}{\mu_{0,i}} \tag{9}$$

where N_{ij} is the coordination number of molecule j around the central molecule/ion i, P_{ij} is the probability molecule i associated to molecule/ion j, while P_i is the probability of molecule i being associated with any other species, γ_{ij} is the angle of the dipole moments of the two hydrogen-bonded molecules, and θ_{ij} is the inner angle of the hydrogen bond structure.

When the ion-water association is not explicitly accounted for within the equations of state, which is common practice, though some recent studies have made attempts to allow explicit associations between water molecules and ions [52,66], Maribo-Mogensen et al. proposed a modification to Equation (7) to account for the association of ion and water molecules [107]

$$\frac{(2\varepsilon_r+\varepsilon_\infty)(\varepsilon_r-\varepsilon_\infty)}{\varepsilon_r(\varepsilon_\infty+2)^2} = \frac{\rho}{9\varepsilon_0 k_B T}\sum_i x_i \Theta_i g_i \mu_{0,i}^2 \tag{10}$$

where Θ_i is the fraction of molecule i that is not bonded (associated) to ions, which can be calculated using the information of hydration numbers. More details can be found in Maribo-Mogensen et al. [107] and Walker et al. [64].

Corresponding to the extended Debye-Hückel theory for activity coefficients of ions, the molar conductivity can be calculated from the Debye-Hückel-Onsager Extended Equation (DHOEE) [2,92]. For a single salt system, it can be written as

$$\Lambda = \Lambda^0 - \left[\frac{N_A e^2}{6\pi\eta}(|Z_+|+|Z_-|) + \frac{|Z_+Z_-|e^2}{12\pi\varepsilon_0\varepsilon_r k_B T}\frac{q}{1+\sqrt{q}}\Lambda^0\right]\frac{\kappa}{1+\kappa\sigma_\pm} \tag{11}$$

where Λ and Λ^0 are the molar conductivity of the system at the specified concentration and the infinite dilution, respectively, and q is equal to 1/2 for the aqueous NaCl solution. More details on predicting of molar conductivity of electrolyte solutions can be found in Boroujeni et al. [92].

3. Results and discussion

3.1. Molecular simulations

3.1.1. Liquid density

The average density (ρ) was calculated using the last 4 ns NPT ensemble simulations by LAMMPS [100]. The simulation results are compared with the experimental data [108], and the simulation data from literature [34,37] in Fig. 1. The deviations of the simulation density in this work from the experimental data and the literature results are lower than 0.5 %, though a slight difference is seen in the qualitative trend.

3.1.2. Self-diffusion coefficient

The self-diffusion coefficient (D) is one of the most common properties investigated in MD simulations. In this work, D is obtained from the equation [110]

$$D_i = \frac{1}{6}\lim_{t\to\infty}\frac{\mathrm{d}}{\mathrm{d}t}\left\langle\frac{1}{n_i}\sum_{j=1}^{n_i}\left|\vec{r}_j(t)-\vec{r}_j(0)\right|^2\right\rangle \tag{12}$$

where $\vec{r}_j(t)$ indicates the positional vector of the center of mass of the j^{th} particle at time t, and n_i is the number of moles of species i. The quantity in <•••> is the mean square displacement (MSD).

Equation (12) is considered valid only when the true diffusive motion is observed. The self-diffusion coefficients obtained by fitting different MSD periods differ greatly, so it is important to know how long the simulation needs to be conducted to compute the MSD and which region is used to fit the self-diffusion coefficient. Cadena *et al.* [111] have argued that the value determined from a too short time MSD usually leads to an overestimation of the self-diffusion coefficients. It is common practice to choose a 'middle' region of the MSD to estimate the self-diffusion coefficients. According to Liu et al. [112], the following variable β was used in this work to determine the diffusive region of ions

$$\beta(t) = \frac{\mathrm{d}}{\mathrm{d}\log(t)}\log\left(\left\langle\frac{1}{n_i}\sum_{j=1}^{n_i}\left|\vec{r}_j(t)-\vec{r}_j(0)\right|^2\right\rangle\right) \tag{13}$$

When the value of β reaches 1, it is considered that the ions have reached a diffusive motion state and that period is good for self-diffusion coefficient estimations. It was found that the ions (Na^+ and Cl^-) did not reach the diffusive regions until about 5.5 ns for all concentrations. Following Maginn et al. [113], therefore, the period of 5.5–6 ns was used for estimating the self-diffusion coefficients.

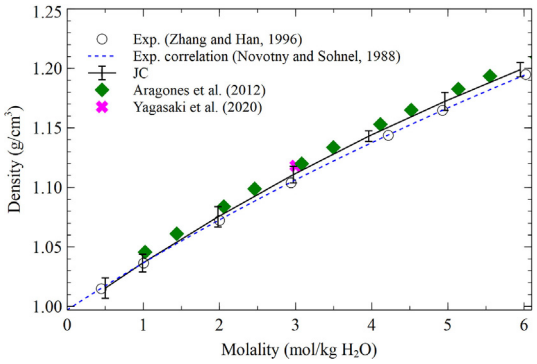

Fig. 1. Density of the aqueous NaCl solutions versus molality at 298 K and 1 bar. Experimental data were taken from Zhang and Han [108] and the Exp. correlation was from Novotny and Sohnel [109]. JC represents the results from this work (the same applies in the following figures). Both Aragones et al. [37] and Yagasaki et al. [34] used the same force field models.

The self-diffusion coefficients of Na^+ and Cl^- and those of H_2O are respectively shown in Fig. 2 and Fig. 3, in which they are compared with the experimental data and other simulation results from literature. It is readily known that all self-diffusion coefficients decrease as the solution gets concentrated, that is, the simulation results and experimental data follow the same trends. The self-diffusion coefficients of ions from simulations are smaller than the experimental values, but they follow similar qualitative trends. The self-diffusion coefficients of H_2O from simulations shows a sharper decrease against concentration than the experimental ones, and they cross each other around 1.5 mol/kg-H_2O. The same qualitative behavior of self-diffusion coefficients was reported by Lyubartsev and Laaksonen [15] with another force filed of ions using both Velocity Autocorrelation Functions and MSD. The JC force field developers Joung and Cheatham reported the simulation results of self-diffusion coefficients of Na^+ and Cl^- at 1 mol/kg-H_2O, with different sizes of the simulation system [35]. The self-diffusion coefficients of ions from this work correspond very closely to their simulation results with larger system sizes, while the more recent simulation results from Yagasaki et al. [34] with the same force field are smaller. Kim et al. made an extensive study on the self-diffusion coefficients of water molecules in electrolyte solutions [36], and the estimated self-diffusion coefficients of H_2O from this work are in excellent agreement with those reported in their simulations using the larger box size. After a comparative molecular dynamics simulation study on the ionic mobilities of Na^+ and Cl^-, Lee [114] concluded that the Ewald sum parameter has a great impact on the simulation results. In a following study, Lee [115] also showed that reasonable self-diffusion coefficients of NaCl could be obtained when an appropriate value of the Ewald sum parameter is chosen, while the best value of this parameter varies as the number of ions in the system changes.

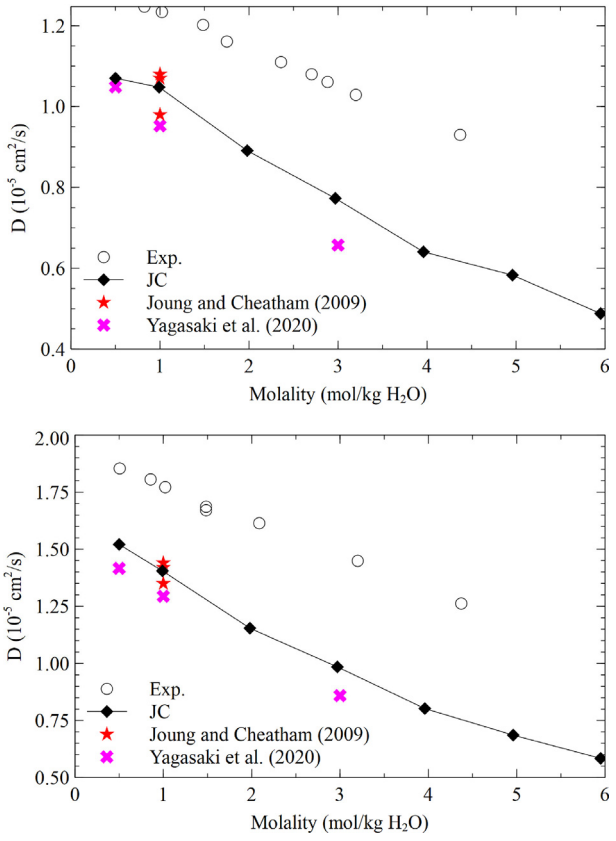

Fig. 2. Self-diffusion coefficient of Na^+ and Cl^- versus concentration. Experimental data were taken from Mills and co-workers [116–119] and Passiniemi [120], and other simulation results were Joung and Cheatham [35] and Yagasaki et al. [34].

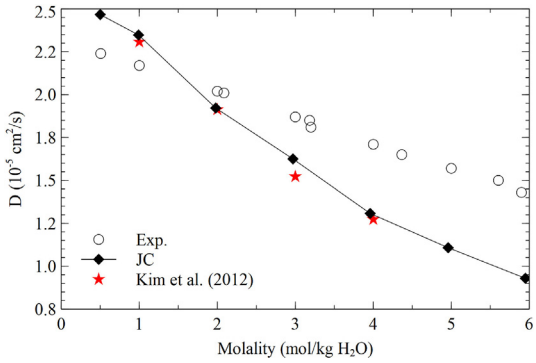

Fig. 3. Self-diffusion coefficient of H_2O versus concentration. Experimental data were taken from Harris et al. [121] and the simulation results were from Kim et al. [36].

It is common practice to correct the simulation system size effect on the self-diffusion coefficient following the approach proposed by Yeh and Hummer [122]

$$D_{\infty,i} = D_i(L) + \frac{k_B T \xi}{6\pi\eta L} \tag{14}$$

where $D_{\infty,i}$ and $D_i(L)$ are the self-diffusion coefficients of species i at infinite size and the simulation box size (L), respectively, ξ accounts for finite-size effects (approximately equal to 2.837297), and η is the shear viscosity.

It is not very clear whether the viscosity of the solvent or that of the solution should be used in Equation (14). It was indicated in the recommendation of best practices for computing transport properties from equilibrium MD simulations [113] that the viscosity of the solution should be used, while Yagasaki et al. [34] clearly stated that the shear viscosity of the solvent should be used. In this work, both approaches have been applied. As shown in Fig. 4, the correction with the shear viscosity of water leads to results closer to the experimental data, but still not accurate enough, especially at high concentrations.

3.1.3. Molar conductivity

The molar conductivity (Λ) measures the efficiency of a solution conducting electricity. The Nernst-Einstein equation [2] is commonly used to relate the self-diffusion coefficients and the molar conductivity. When the motion of the ions within an electrolyte solution is uncorrelated, this equation shows that the ionic mobility is proportional to the self-diffusion coefficient (D_i):

$$\Lambda_{NE} = \frac{N_A e^2}{k_B T} \sum_i \nu_i Z_i^2 D_i \tag{15}$$

In principle, this relation is only valid at infinite dilution. As seen from Fig. 5, the experimental molar conductivity and the calculated ones via Equation (15) from the experimental self-diffusion coefficients, high-order polynomials applied for fitting the data shown in Fig. 2, meet perfectly at the limiting zero concentration, while they diverge quickly (more than 2 % deviation already from 0.002 mol/kg H_2O). It is surprising, though, to see that the self-diffusion coefficients predicted from simulations give very reasonable values of molar conductivity, for example below 3 mol/kg H_2O. It would be interesting to figure out whether this is merely a coincidence due to error cancellation or there are some fundamental explanations.

In a long series of works, Harris, Hertz, Mills and their colleagues [123–126] had proposed and developed the concept of velocity (cross-)correlation coefficients to improve the Nernst-Einstein relation, which can be summarized as [127]

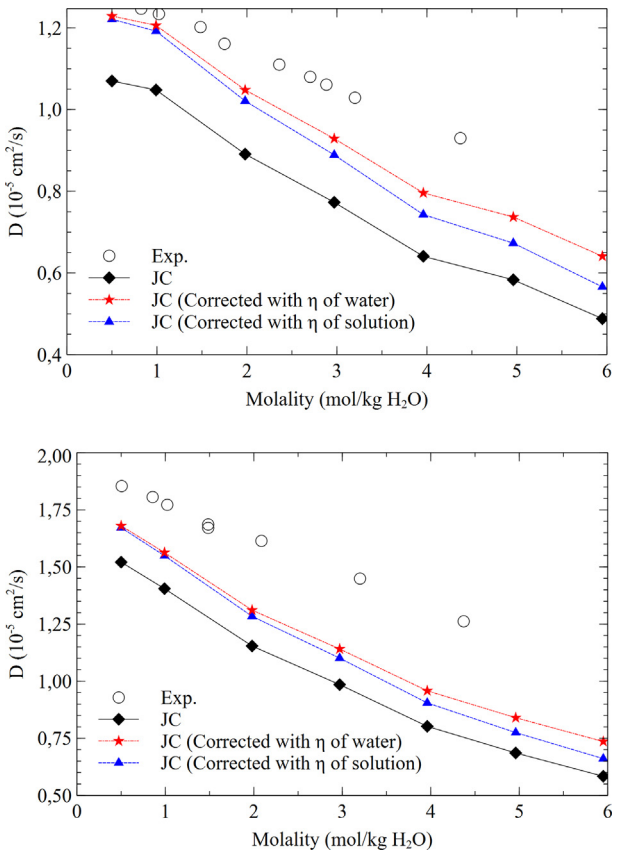

Fig. 4. Self-diffusion coefficient of Na^+ (Top) and Cl^- (Bottom) versus concentration, comparison with corrections of the simulation system size using either the viscosity of water or the solution. The references for the experimental data are given in Fig. 2.

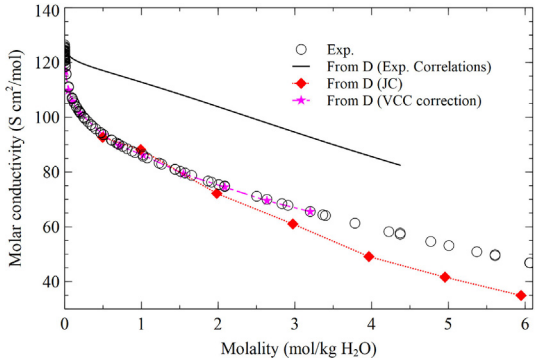

Fig. 5. Molar conductivity versus molality, comparison among experimental data [129–137], calculated results from experimental and simulated self-diffusion coefficients via Equation (15), and calculated results from experimental self-diffusion coefficients with correction using velocity (cross-)correlation coefficients via Equation (16) [127].

$$\Lambda = \Lambda_{NE}(1 - \Delta) \tag{16}$$

For the aqueous solution of NaCl, the deviation Δ was calculated from

$$\Delta = \frac{2f_{12} - f_{11} - f_{22}}{D_1/v_1 + D_2/v_2} \tag{17}$$

where the values of f_{12}, f_{11} and f_{22} are from Woolf and Harris [125].

The velocity (cross-)correlation coefficients were given for aqueous NaCl solutions from 0.01 to 3 mol/L. It is worth mentioning that the values given in the relevant tables shall be directly used, that is, the Asterix (Asterisk) given for f_{12}, f_{11} and f_{22} in those tables shall be omitted, according to the follow-up correction [128]. The corrected molar conductivity from the self-diffusion coefficients following Equation (16) is also shown in Fig. 5. There is no doubt that it is a very successful method. It is also worth noting that, instead of individual self-diffusion coefficients, Lyubartsev and Laaksonen [15] applied the interdiffusion coefficient in the Nernst-Einstein equation, which shared the same characteristic of Equation (16), and they obtained molar conductivity with values lower than the experimental ones.

3.1.4. Radial distribution function

The radial distribution function (RDF) plays an important role in liquid-state physics, for instance for studying the structure of liquids and solutions. RDF describes the spherically averaged local organization around any given atom. It is common practice to use the site-site RDF of $Na^+ - O^-$ and $Cl^- - O^-$ to study the structural information of ions and water [15,17,34]. Fig. 6 presents some site-site RDF curves at different concentrations (the molality numbers given in the legends are approximate ones, as explained in the section of Methods).

It is apparent that the concentration does not have an impact on the positions of the first maximum and minimum peak points, for which a similar behavior was reported by Ghaffari and Rahbar-Kelishami [138] with a different ion model. The first maximum peak points of the RDF of $Na^+ - O^-$ and that of $Cl^- - O^-$ are allocated at 2.37–2.38 Å and 3.13 Å, respectively, which are almost exactly the same values reported by Joung and Cheatham [35] and Yagasaki et al. [34]. The first minimum peak points of these two RDF curves are at 3.17 Å ($Na^+ - O^-$) and 3.81 Å ($Cl^- - O^-$), which are slightly lower than those (3.19 Å and 3.86 Å, respectively) given

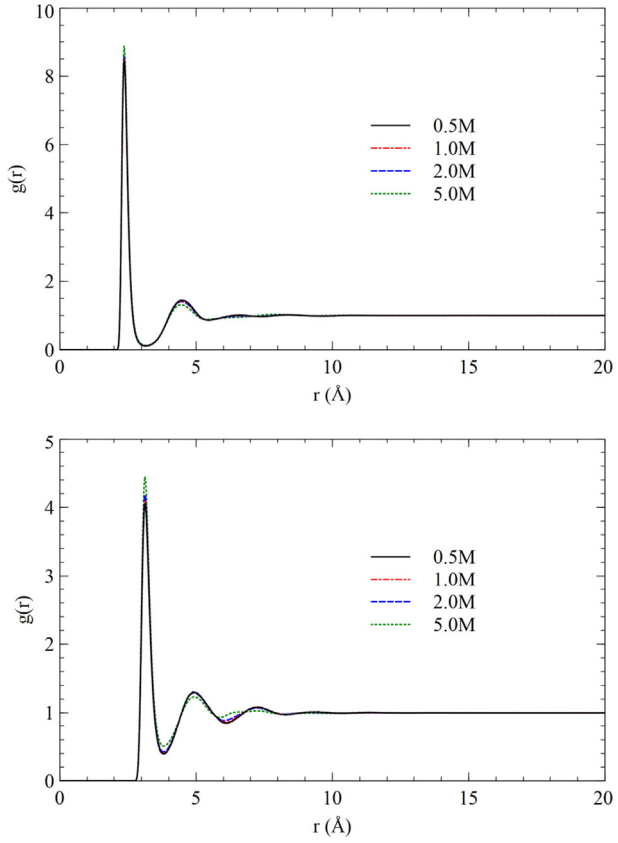

Fig. 6. The RDF curves of $Na^+ - O^-$ (Top) and those of $Cl^- - O^-$ (Bottom) at different concentrations.

by Joung and Cheatham [35]. The peak values increase as the solution gets concentrated, which is more pronounced for the case of the RDF of Cl^- – O^-.

Fig. 7 presents the RDF of Na^+ – Cl^- at 1 mol/kg H_2O and 5 mol/kg H_2O, and it also contains the corresponding RDF with the same force fields at 4.9 mol/kg H_2O, digitalized from Saravi and Panagiotopoulos [41]. Apparently, simulation results from both studies are in excellent agreement to each other. It is also observed that the first maximum and minimum peak points, even the second maximum peak point to some extent, are essentially not affected by the concentration, which is the same behavior seen in the RDF of ions and (the Oxygen atom of) water molecules. The first maximum and minimum peak points are allocated at 2.81–2.83 Å and 3.51 Å, respectively, which are essentially the same values reported by Joung and Cheatham [35]. A similar conclusion was given by Benavides et al. [26] from a study on a force field model for the aqueous NaCl solution based on another water model. A significant difference of the RDF of Na^+ – Cl^-, compared with those of ions and water molecules, is that the first maximum peak, corresponding to the contact ion pairs, is lower than the second maximum peak which corresponds to the solvent-separated ion pairs. Another noticeable difference is that the concentration has a larger impact on the maximum peak values. As concentration increases, on one hand, the first maximum peak and the second maximum peak become larger and smaller, respectively. This implies that Na^+ and Cl^- tend to form contact ion pairs easier at higher concentrations, which might be partially responsible for the decrease of the self-diffusion coefficients of ions, as shown in Fig. 2. It shall be emphasized, however, that the solvent-separate ion pairs are still more significant at higher concentrations. On the other hand, the value of the first minimum peak has practically not changed.

3.1.5. Coordination number

The average number of water molecules around a given ion and the number of contact ion pairs can be obtained from the so-called coordination number, which is identified by integrating the RDF up to the first minimum peak (the first solvation shell)

$$N_{ij} = 4\pi\rho_j \int_0^{R_{1\min}} g_{ij}(r) r^2 \mathrm{d}r \tag{18}$$

where $R_{1\min}$ is the first minimum peak position of the corresponding RDF (first solvation shell radius), r is the distance, and ρ_j is the number density of species j.

The coordination numbers of the RDF of Na^+ – O^- and Cl^- – O^-, also known as hydration numbers of ions Na^+ and Cl^-, are presented in Fig. 8. Even though the hydration numbers of Na^+ and Cl^- respectively, very slightly, decrease and increase as the solution gets concentrated, in reality they can be considered practically unchanged. The average hydration numbers of Na^+ and Cl^- are 5.8 ± 0.07 and 7.2 ± 0.06, respectively. These values match accurately with the numbers reported by Joung and Cheatham [35] and Yagasaki et al. [34].

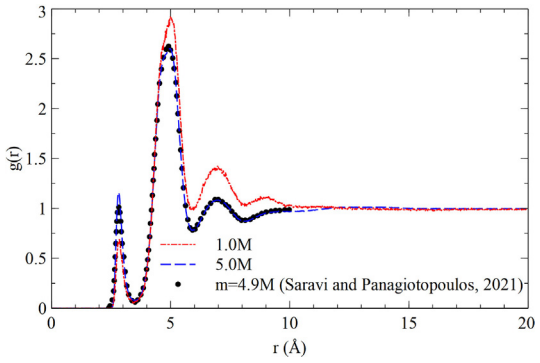

Fig. 7. The RDF curves of Na^+ – Cl^- at different concentrations, compared to literature [41].

The coordination numbers of the RDF of Na^+ – Cl^-, also known as the number of ion pairs, are plotted in Fig. 9. Unlike the hydration numbers of ions, the number of ion pairs increases much more rapidly when the concentration gets higher, which is also indicated in the RDF of Na^+ – Cl^- from Fig. 7. As seen from Fig. 9, the results from this work are in good agreement with literature data [33,35].

3.2. Molecular theories

3.2.1. Gibbs energy of solvation

When the first shell solvation radius is known, the Gibbs energy of solvation can be predicted using the Born equation, given in equation (2). Therefore, the first shell solvation radius used in this context is often called Born radius. The calculated Gibbs energies of solvation of Na^+ and Cl^- using the static relative permittivity of water from molecular simulations (73.3) and from experimental data (78.49) [42] are compared with the experimental data from literature in Table 1. Noticeable deviations can be seen among these experimental data, up to 15–20 %. The values reported by Fawcett [139] have been widely used in molecular theories and models [50,104,105], while Joung and Cheatham [17] chose to use the data from Schmid [140] for parameter optimization of the force fields. It is interesting to see that the predicted Gibbs energy of solvation of Na^+ matches the experimental data reported by Fawcett [139] accurately, while the estimated Gibbs energy of solvation of Cl^- is much closer to the one report by Schmid [140]. The Gibbs energy of solvation is the Gibbs energy change for the process of transferring an ion from vacuum to solvent. As very nicely discussed in detail by Joung and Cheatham [17], numerous experimental values of Gibbs energy of solvation had been reported for individual ions, under different assumptions how to decompose the energies of electrolytes into ions, while none of the approaches has been able to get fully validated or assessed. More discussion can be found in Joung and Cheatham and the literature cited there [17]. Therefore, the predicted Gibbs energy of solvation with the Born equation can be considered overall satisfactory, which indicates that the Born radii (the first solvation shell radii) from molecular simulations are reasonable. More importantly, these Born radii essentially do not change with concentration, as discussed above, which makes it convenient when they are used in molecular theories and models. The static relative permittivity of water might be largely affected by the setup in simulations or the use of different force fields [30], while it is also worth noticing that the value of the static relative permittivity of the solvent has a much smaller effect than the Born radii, as seen in Table 1. This is also consistent with the statement given by Hummer et al. [141], who made extensive studies on the Gibbs energy of solvation from molecular simulations.

3.2.2. Static relative permittivity

The static relative permittivity of the solution was predicted using the theory of Maribo-Mogensen et al. [107], as summarized in Section 2.2. The basic properties and parameters of ions and water were taken from Maribo-Mogensen et al. [106], and the average hydration numbers of water molecules around ions are from this work (Section 3.1.5). The values are listed in Table 2. The average association probability of water molecules at the given condition, needed in Equation (9), was calculated from the SAFT-VR Mie equation of state following the approach reported by Walker et al. [64]. The required parameters are given in Table 3, which contains the SAFT-VR Mie parameters for water [64], and also the JC ion model parameters of Na^+ and Cl^- [17]. Water mole-

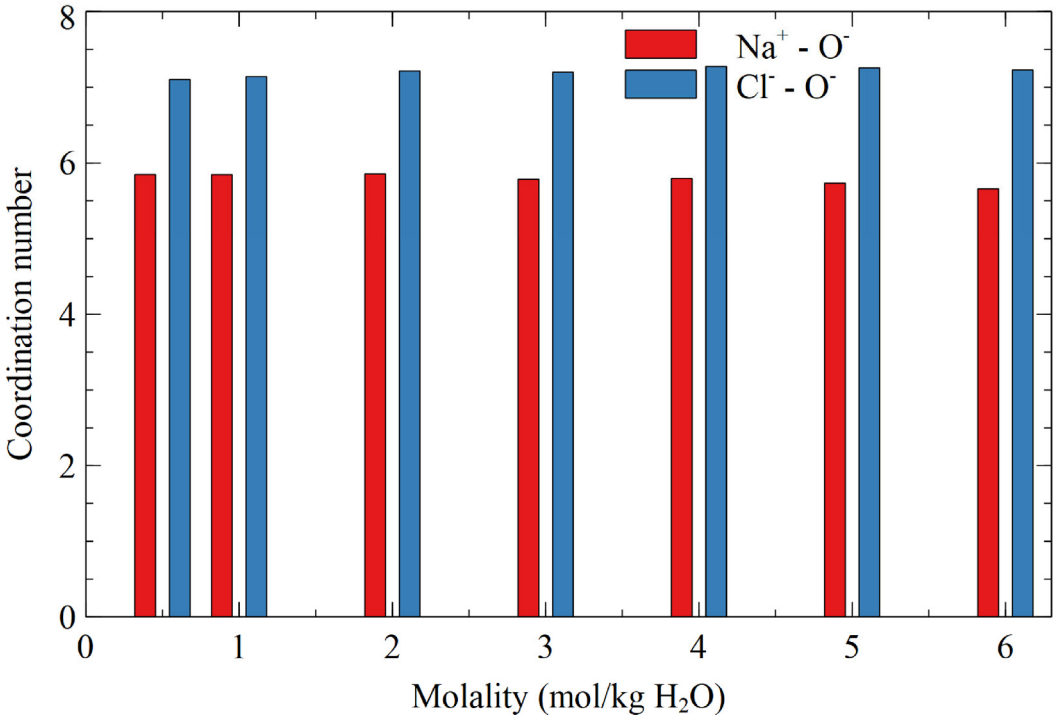

Fig. 8. The coordination numbers of Na^+ – O^- and Cl^- – O^- versus concentration.

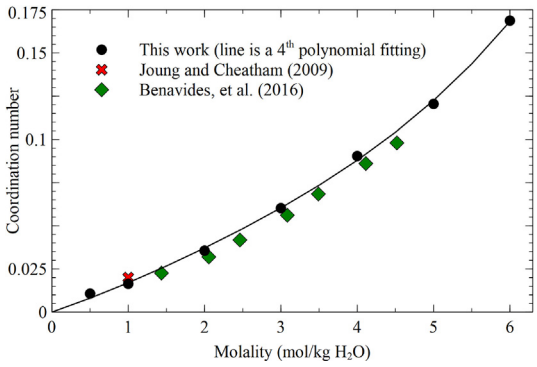

Fig. 9. The coordination numbers of Na^+ – Cl^- versus concentration, compared with literature results from Joung and Cheatham [35] and Benavides et al. [33].

cules and ions are all assumed spheres, which means the length of the species is 1, and ions are also assumed non-associating. The details of the calculations with regard to the SAFT-VR Mie equation of state as well as the prediction of the static relative permittivity of an electrolyte solution can be found from Walker et al. [64]. The required density is either from molecular simulations or experimental data.

The predicted static relative permittivity values are compared with experimental data, correlations and simulation results from literature in Fig. 10. It is worth mentioning that noticeable deviations are seen among experimental data from different literature sources [143,144], even more than 30 % at high concentrations. The predicted results from molecular theories and molecular simulations are respectively larger and smaller than the experimental data, and apparently both of them follow a clear decreasing trend as the concentration increases. As discussed above, the simulated

Table 1
Comparison of the Gibbs energies of solvation estimated in this work and the experimental data from literature.

Ion	R_{1min}(Å) (with H_2O)	ΔG_i^s(kJ/mol)				
		Estimation using Equation (2)		Experimental data		
		ε_w(sim.)	ε_w(exp.)	Schmid [140]	Marcus [142]	Fawcett [139]
Na^+	3.17	432.3	432.7	370.8	364.5	424.0
Cl^-	3.81	359.7	360.0	373.3	339.8	304.0

Table 2
Key parameters for calculating the static relative permittivity * [106].

Species	μ_0(Debye)	$\alpha_0 \times 10^{40}$(C^2m^2/J)	θ_{ij}(degree)	γ_{ij}(degree)	N_{ij}(with H_2O)
H_2O	1.855	1.613	109.5	69.4	4
Na^+	0	2.221	0	0	5.8
Cl^-	0	3.557	0	0	7.2

* All the parameters were taken from Maribo-Mogensen et al. [106], except for the hydration numbers of the ions, which are from the molecular simulations in this work (Section 3.1.5).

Table 3
Parameters of water and ions used in the SAFT-VR Mie equation of state [17,64].

Species	Z	λ_r	λ_a	ϵ/R(K)	σ(Å)	ϵ^{AB}/R(K)	K^{AB}(Å^3)
H_2O	0	17.02	6	266.68	3.0063	1985.4	101.69
Na^+	+1	12	6	177.14	2.159	0	0
Cl^-	−1	12	6	6.345	4.830	0	0

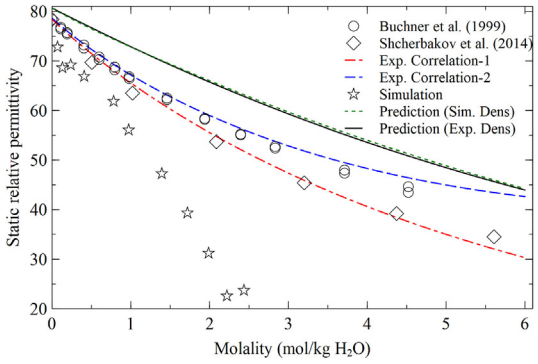

Fig. 10. Static relative permittivity versus concentration, comparison among experimental data [143,144], correlations [145], simulations [42] and theory predictions [107] with different density, either from simulation (Sim. Dens) or experiment (Exp. Dens).

density is very close to the experimental data (Fig. 1), so it is not surprising to see that the theory predicts almost the same static relative permittivity values using these two sets of density. The experimental correlation of density [109] was used in the following calculations.

The effect (sensitivity) of hydration numbers in Equations (9) and (10) has been studied and the results are presented in Fig. 11. The hydration numbers of 6 and 5 water molecules respectively around Na^+ and Cl^- were from Maribo-Mogensen et al. [107], while the other two combinations are round numbers from the actual values obtained in this work. It can be seen that the effect of hydration numbers is overall moderate, with difference up to 10 % at high concentrations.

3.2.3. Mean ionic activity coefficient

The mean ionic activity coefficient was predicted with the extended Debye-Hückel theory, Equation (3), using the average size parameters of ions (usually called the distance of closest approach, (2.159 + 4.830) / 2 = 3.4945 Å). In these calculations, we used two salt concentration dependent static relative permittivity curves predicted in the previous section (3.2.2) with different hydration numbers. This investigation can show how the impact of parameters used in predicting the static relative permittivity is transferred to the prediction of other properties. In the meantime, it can also tell the importance of using the right parameters for more accurate predictions. The results are presented in Fig. 12. It is remarkable to see that the mean ionic activity coefficient can be predicted very accurately, with the most stable information merely from molecular simulations plus some basic properties of water and ions. The average deviation of the prediction is 1.1 %, with a maximum deviation smaller than 8 % up to 6 mol/kg H_2O. This calculation suggests that the actual hydration numbers from molecular simulations should be used when they are available. Otherwise, higher deviations are obtained. The fact that the predicted static relative permittivity is larger than the experimental data, as seen from Figs. 10 and 11, may somewhat reflect the ongoing debated topic whether there is a kinetic depolarization contribution which cannot be captured by molecular thermodynamic theories, and shall not be included in thermodynamic modeling [12]. The mean ionic activity coefficients predicted directly from recent molecular dynamics simulations with the same force fields are added for comparison. It needs to be pointed out that the simulation results shown in Fig. 12 are the average values, and the uncertainty may vary from about 30 % to 80 % at different salt concentrations [41].

3.2.4. Molar conductivity

The molar conductivity was predicted with the Debye-Hückel-Onsager extended equation, Equation (11), using the viscosity of water (0.8909 mPa-s) [148], the average size parameters of ions (or the distance of closest approach, 3.4945 Å) and the molar conductivity at infinite dilution (50.08 and 76.31 S-cm^2/mol for Na^+ and Cl^-, respectively [92]). The results are presented in Fig. 13, in which different approaches of the static relative permittivity has been applied. The studied approaches include the static relative permittivity values of water from molecular simulations and experimental data, as well as those predicted in the previous section using the theory of Maribo-Mogensen et al. [106,107] with

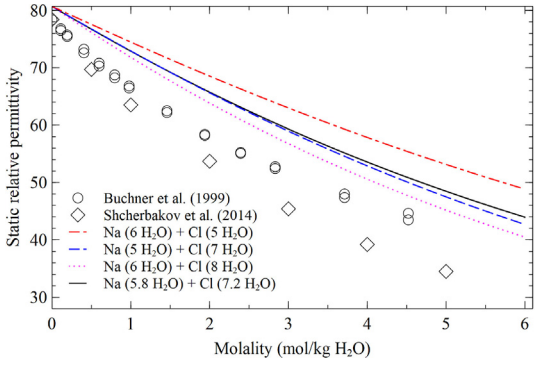

Fig. 11. Sensitivity of hydration numbers on the static relative permittivity prediction. The first combination of hydration numbers was from Maribo-Mogensen et al. [107], while the other two combinations are round numbers from the actual values (5.8 and 7.2 obtained in Section 3.1.5).

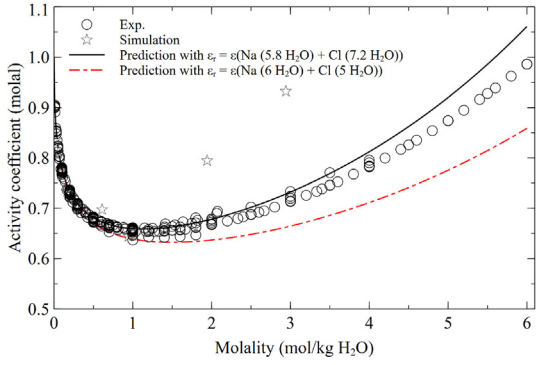

Fig. 12. Comparison of the predicted mean ionic activity coefficients from the extended Debye-Hückel equation using two different static relative permittivity curves from Fig. 11 with the experimental data [146,147] and simulation results [41].

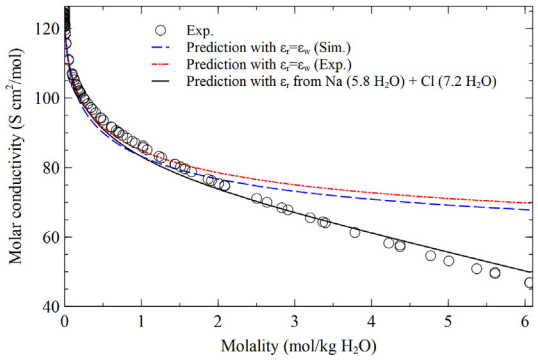

Fig. 13. Molar conductivity versus concentration predicted from the Debye-Hückel-Onsager extended equation. The static relative permittivity in the solid line is predicted using the theory of Maribo-Mogensen et al. [106,107] with rigorous coordination numbers (the black line in Fig. 10 and Fig. 11), while the other two are constants (either from simulations or experiment [42]). The references for the experimental data can be found in the caption of Fig. 5.

the rigorous coordination numbers (that is, the black line in Fig. 10 and Fig. 11). It can be concluded that the static relative permittivity value of water has a minor effect on the results, and they can be used for satisfactory predictions below 2 mol/kg-H_2O, while a salt concentration dependent static relative permittivity is very important for high concentration regions. It is again remarkable to see that such an accurate prediction, with an average deviation of 1.4 % and the largest deviation smaller than 7 % up to 6 mol/kg H_2O, is obtained.

4. Conclusions

In this work, molecular dynamics simulations and molecular theories were used to predict various properties of the aqueous sodium chloride solutions. With the SPC/E water model and JC ion model, it is found that the solution density can be predicted very accurately, lower than 0.5 %, with molecular dynamics simulations. The self-diffusion coefficients of ions are underpredicted, while the qualitative behavior is very reasonable. However, the self-diffusion coefficients of water molecules are quantitatively satisfactory from low to medium concentrations, while the predicted ones present a quicker decrease as the concentration increases. Using the Nernst-Einstein equation, the self-diffusion coefficients predicted from simulations can give very accurate molar conductivity below 3 mol/kg H_2O. By analyzing the radial distribution functions of ion-ion and ion-water, it is found that the first shell solvation radii and coordination numbers of ions are practically not changed with concentration. With the first shell solvation radii, the Gibbs energy of solvation can be predicted very satisfactorily, within the errors among the experimental data reported in literature. Using the JC ion model parameters and the coordination numbers from simulations, the static relative permittivity is overpredicted compared to experimental data of a somewhat high uncertainty. However, the mean ionic activity coefficients and molar conductivity can be predicted very accurately, lower than 1.5 %, in the entire range of concentrations (up to 6 mol/kg H_2O), using this overpredicted static relative permittivity. This may somewhat reflect an on-going debated topic that there is a kinetic depolarization contribution which cannot be captured by molecular thermodynamic theories, and it shall probably not be included in thermodynamic modeling.

CRediT authorship contribution statement

Jiahuan Tong: Conceptualization, Methodology, Writing – original draft, Data curation. **Baoliang Peng:** Conceptualization, Methodology, Writing – review & editing, Funding acquisition. **Georgios M. Kontogeorgis:** Conceptualization, Methodology, Writing – review & editing, Supervision, Funding acquisition. **Xiaodong Liang:** Conceptualization, Methodology, Writing – review & editing, Supervision, Funding acquisition.

Data availability

Data will be made available on request.

Declaration of Competing Interest

The authors declare that they have no known competing financial interests or personal relationships that could have appeared to influence the work reported in this paper.

Acknowledgement

The authors wish to thank the European Research Council (ERC) for funding this research under the European Union's Horizon 2020 research and innovation program (grant agreement no 832460), ERC Advanced Grant project "New Paradigm in Electrolyte Thermodynamics". The authors also wish to thank the Scientific Research and Technology Development Project of RIPED, PetroChina (YGJ2019-11-01) for funding this research. Dr. Baoliang Peng wishes to thank the National Natural Science Foundation of China (22008263) for funding this research.

References

[1] J.M. Prausnitz, R.N. Lichtenthaler, E.G. de Azevedo, Molecular thermodynamics of fluid-phase equilibria, Pearson Education, 1998.
[2] R.A. Robinson, R.H. Stokes, Electrolyte solutions, Courier Corporation, 2002.
[3] G.M. Kontogeorgis, G.K. Folas, Thermodynamic models for industrial applications: from classical and advanced mixing rules to association theories, John Wiley & Sons, 2009.
[4] J.F. Zemaitis Jr, D.M. Clark, M. Rafal, N.C. Scrivner, Handbook of aqueous electrolyte thermodynamics: Theory & application, John Wiley & Sons, 2010.
[5] U. von Stockar, L. van der Wielen, Biothermodynamics, EPFL Press, 2013.
[6] V.A. Azov, K.S. Egorova, M.M. Seitkalieva, A.S. Kashin, V.P. Ananikov, Solvent-in-Salt Systems for Design of New Materials in Chemistry, Biology and Energy Research, Chem. Soc. Rev. 47 (2018) 1250–1284, https://doi.org/10.1039/c7cs00547d.
[7] H.J. Bakker, Structural dynamics of aqueous salt solutions, Chem. Rev. 108 (2008) 1456–1473, https://doi.org/10.1021/cr0206622.
[8] F. Moučka, I. Nezbeda, W.R. Smith, Molecular force fields for aqueous electrolytes SPCE compatible charged LJ, J. Chem.. Phys. 138 (2013), https://doi.org/10.1063/1.4801322.
[9] I. Nezbeda, F. Moučka, W.R. Smith, Recent progress in molecular simulation of aqueous electrolytes: Force fields, chemical potentials and solubility, Mol. Phys. 114 (2016) 1665–1690.
[10] W.R. Smith, I. Nezbeda, J. Kolafa, F. Moučka, Recent progress in the molecular simulation of thermodynamic properties of aqueous electrolyte solutions, Fluid Phase Equilib. 466 (2018) 19–30.
[11] G.M. Kontogeorgis, B. Maribo-Mogensen, K. Thomsen, The Debye-Hückel theory and its importance in modeling electrolyte solutions, Fluid Phase Equilib. 462 (2018) 130–152.
[12] G.M. Kontogeorgis, A. Schlaikjer, M.D. Olsen, B. Maribo-Mogensen, K. Thomsen, N. von Solms, X. Liang, A Review of Electrolyte Equations of State with Emphasis on Those Based on Cubic and Cubic-Plus-Association (CPA) Models, Int J Thermophys. 43 (2022) 1–68.
[13] A.Z. Panagiotopoulos, Simulations of activities, solubilities, transport properties, and nucleation rates for aqueous electrolyte solutions, J. Chem. Phys. 153 (2020) 10903.
[14] D.E. Smith, L.X. Dang, Computer simulations of NaCl association in polarizable water, J. Chem. Phys. 100 (1994) 3757–3766, https://doi.org/10.1063/1.466363.
[15] A.P. Lyubartsev, A. Laaksonen, Concentration Effects in Aqueous NaCl Solutions. A Molecular Dynamics Simulation, J. Phys. Chem. 100 (40) (1996) 16410–16418.
[16] G. Lamoureux, B. Roux, Absolute Hydration Free Energy Scale for Alkali and Halide Ions Established from Simulations with a Polarizable Force Field, J. Phys. Chem. B 110 (2006) 3308–3322, https://doi.org/10.1021/jp056043p.
[17] I.S. Joung, T.E. Cheatham, Determination of alkali and halide monovalent ion parameters for use in explicitly solvated biomolecular simulations, J. Phys. Chem. B 112 (30) (2008) 9020–9041.

[18] D. Horinek, S.I. Mamatkulov, R.R. Netz, Rational design of ion force fields based on thermodynamic solvation properties, J. Chem. Phys. 130 (2009).
[19] H. Yu, T.W. Whitfield, E. Harder, G. Lamoureux, I. Vorobyov, V.M. Anisimov, A. D. MacKerell, B. Roux, Simulating Monovalent and Divalent Ions in Aqueous Solution Using a Drude Polarizable Force Field, J. Chem. Theory Comput. 6 (3) (2010) 774–786.
[20] M.M. Reif, P.H. Hünenberger, Computation of methodology-independent single-ion solvation properties from molecular simulations. IV. Optimized Lennard-Jones interaction parameter sets for the alkali and halide ions in water, J. Chem. Phys. 134 (2011).
[21] S. Deublein, J. Vrabec, H. Hasse, A set of molecular models for alkali and halide ions in aqueous solution, J. Chem. Phys. 136 (2012) 84501, https://doi.org/10.1063/1.3687238.
[22] P.T. Kiss, A. Baranyai, A systematic development of a polarizable potential of water, J. Chem. Phys. 138 (2013), https://doi.org/10.1063/1.4807600.
[23] P.T. Kiss, A. Baranyai, A new polarizable force field for alkali and halide ions, J. Chem. Phys. 141 (2014), https://doi.org/10.1063/1.4895129.
[24] J. Kolafa, Solubility of NaCl in water and its melting point by molecular dynamics in the slab geometry and a new BK3-compatible force field, J. Chem. Phys. 145 (2016), https://doi.org/10.1063/1.4968045.
[25] R. Fuentes-Azcatl, M.C. Barbosa, Sodium Chloride, NaCl/ϵ: New Force Field, J. Phys. Chem. B 120 (2016) 2460–2470, https://doi.org/10.1021/acs.jpcb.5b12584.
[26] A.L. Benavides, M.A. Portillo, V.C. Chamorro, J.R. Espinosa, J.L.F. Abascal, C. Vega, A potential model for sodium chloride solutions based on the TIP4P/2005 water model, J. Chem. Phys. 147 (2017).
[27] C. Zhang, F. Giberti, E. Sevgen, J.J. de Pablo, F. Gygi, G. Galli, Dissociation of salts in water under pressure, Nat. Commun. 11 (2020) 3037, https://doi.org/10.1038/s41467-020-16704-9.
[28] H.J.C. Berendsen, J.R. Grigera, T.P. Straatsma, The missing term in effective pair potentials, J. Phys. Chem. 91 (1987) 6269–6271, https://doi.org/10.1021/j100308a038.
[29] Y. Guissani, B. Guillot, A computer simulation study of the liquid-vapor coexistence curve of water, J. Chem. Phys. 98 (1993) 8221–8235, https://doi.org/10.1063/1.464527.
[30] D. van der Spoel, P.J. van Maaren, H.J.C. Berendsen, A systematic study of water models for molecular simulation: Derivation of water models optimized for use with a reaction field, J. Chem. Phys. 108 (1998) 10220–10230, https://doi.org/10.1063/1.476482.
[31] B. Guillot, A reappraisal of what we have learnt during three decades of computer simulations on water, J. Mol. Liq. 101 (2002) 219–260, https://doi.org/10.1016/S0167-7322(02)00094-6.
[32] I. Shvab, R.J. Sadus, Atomistic water models: Aqueous thermodynamic properties from ambient to supercritical conditions, Fluid Phase Equilib. 407 (2016) 7–30, https://doi.org/10.1016/j.fluid.2015.07.040.
[33] A.L. Benavides, J.L. Aragones, C. Vega, Consensus on the solubility of NaCl in water from computer simulations using the chemical potential route, J. Chem. Phys. 144 (2016), https://doi.org/10.1063/1.4943780.
[34] T. Yagasaki, M. Matsumoto, H. Tanaka, Lennard-Jones Parameters Determined to Reproduce the Solubility of NaCl and KCl in SPC/E, TIP3P, and TIP4P/2005 Water, J. Chem. Theory Comput. 16 (2020) 2460–2473, https://doi.org/10.1021/acs.jctc.9b00941.
[35] I.S. Joung, T.E. Cheatham, Molecular dynamics simulations of the dynamic and energetic properties of alkali and halide ions using water-model-specific ion parameters, J. Phys. Chem. B 113 (40) (2009) 13279–13290.
[36] J.S. Kim, Z. Wu, A.R. Morrow, A. Yethiraj, A. Yethiraj, Self-Diffusion and Viscosity in Electrolyte Solutions, J. Phys. Chem. B 116 (2012) 12007–12013, https://doi.org/10.1021/jp306847t.
[37] J.L. Aragones, E. Sanz, C. Vega, Solubility of NaCl in water by molecular simulation revisited, J. Chem. Phys. 136 (2012), https://doi.org/10.1063/1.4728163.
[38] G.A. Orozco, O.A. Moultos, H. Jiang, I.G. Economou, A.Z. Panagiotopoulos, Molecular simulation of thermodynamic and transport properties for the H2O+NaCl system, J. Chem. Phys. 141 (2014), https://doi.org/10.1063/1.4903928.
[39] Z.R. Kann, J.L. Skinner, A scaled-ionic-charge simulation model that reproduces enhanced and suppressed water diffusion in aqueous salt solutions, J. Chem. Phys. 141 (2014), https://doi.org/10.1063/1.4894500.
[40] H. Jiang, A. Haji-Akbari, P.G. Debenedetti, A.Z. Panagiotopoulos, Forward flux sampling calculation of homogeneous nucleation rates from aqueous NaCl solutions, J. Chem. Phys. 148 (2018), https://doi.org/10.1063/1.5016554.
[41] S.H. Saravi, A.Z. Panagiotopoulos, Individual Ion Activity Coefficients in Aqueous Electrolytes from Explicit-Water Molecular Dynamics Simulations, J. Phys. Chem. B 125 (2021) 8511–8521, https://doi.org/10.1021/acs.jpcb.1c04019.
[42] S.H. Saravi, A.Z. Panagiotopoulos, Activity coefficients of aqueous electrolytes from implicit-water molecular dynamics simulations, J. Chem. Phys. 155 (2021), https://doi.org/10.1063/5.0064963.
[43] C. Held, Thermodynamic gEModels and Equations of State for Electrolytes in a Water-Poor Medium: A Review, J. Chem. Eng. Data 65 (2020) 5073–5082, https://doi.org/10.1021/acs.jced.0c00812.
[44] P.M. May, D. Rowland, Thermodynamic Modeling of Aqueous Electrolyte Systems: Current Status, J. Chem. Eng. Data 62 (2017) 2481–2495, https://doi.org/10.1021/acs.jced.6b01055.
[45] G.M. Kontogeorgis, X. Liang, A. Arya, I. Tsivintzelis, Equations of state in three centuries. Are we closer to arriving to a single model for all applications?, Chem Eng. Sci. X. 7 (2020), https://doi.org/10.1016/j.cesx.2020.100060.
[46] J. Rozmus, J.-C. de Hemptinne, A. Galindo, S. Dufal, P. Mougin, Modeling of strong electrolytes with ePPC-SAFT up to high temperatures, Ind. Eng. Chem. Res. 52 (29) (2013) 9979–9994.
[47] X. Courtial, N. Ferrando, J.C. de Hemptinne, P. Mougin, Electrolyte CPA equation of state for very high temperature and pressure reservoir and basin applications, Geochim. Cosmochim. Acta 142 (2014) 1–14, https://doi.org/10.1016/j.gca.2014.07.028.
[48] J.M.A. Schreckenberg, S. Dufal, A.J. Haslam, C.S. Adjiman, G. Jackson, A. Galindo, Modelling of the thermodynamic and solvation properties of electrolyte solutions with the statistical associating fluid theory for potentials of variable range, Mol. Phys. 112 (17) (2014) 2339–2364.
[49] B. Maribo-mogensen, K. Thomsen, G.M. Kontogeorgis, An Electrolyte CPA Equation of State for Mixed Solvent Electrolytes, (n.d.).
[50] D.K. Eriksen, G. Lazarou, A. Galindo, G. Jackson, C.S. Adjiman, A.J. Haslam, Development of intermolecular potential models for electrolyte solutions using an electrolyte SAFT-VR Mie equation of state, Mol. Phys. 114 (2016) 2724–2749, https://doi.org/10.1080/00268976.2016.1236221.
[51] G. Das, S. Hlushak, C. McCabe, A SAFT-VR+DE equation of state based approach for the study of mixed dipolar solvent electrolytes, Fluid Phase Equilib. 416 (2016) 72–82, https://doi.org/10.1016/j.fluid.2015.11.027.
[52] R. Shahriari, M.R. Dehghani, Prediction of thermodynamic properties of aqueous electrolyte solutions using equation of state, AIChE J 63 (11) (2017) 5083–5097.
[53] M.A. Selam, I.G. Economou, M. Castier, A thermodynamic model for strong aqueous electrolytes based on the eSAFT-VR Mie equation of state, Fluid Phase Equilib. 464 (2018) 47–63.
[54] J.P. Simonin, On the solution of the mean-spherical approximation (MSA) for ions in a dipolar solvent in the general case, AIP Adv. 10 (2020), https://doi.org/10.1063/5.0022864.
[55] M. Bülow, X. Ji, C. Held, Incorporating a concentration-dependent dielectric constant into ePC-SAFT, An application to binary mixtures containing ionic liquids, Fluid Phase Equilib. 492 (2019) 26–33, https://doi.org/10.1016/j.fluid.2019.03.010.
[56] S. Ahmed, N. Ferrando, J.C. de Hemptinne, J.P. Simonin, O. Bernard, O. Baudouin, Modeling of mixed-solvent electrolyte systems, Fluid Phase Equilib. 459 (2018) 138–157, https://doi.org/10.1016/j.fluid.2017.12.002.
[57] L.i. Sun, X. Liang, N.V. Solms, G.M. Kontogeorgis, Analysis of some electrolyte models including their ability to predict the activity coefficients of individual ions, Ind. Eng. Chem. Res. 59 (25) (2020) 11790–11809.
[58] J.P. Simonin, On the "born" term used in thermodynamic models for electrolytes, J. Chem. Phys. 150 (2019), https://doi.org/10.1063/1.5096598.
[59] M. Theiss, J. Gross, Nonprimitive Model Electrolyte Solutions: Comprehensive Data from Monte Carlo Simulations, J. Chem. Eng. Data 65 (2020) 634–639, https://doi.org/10.1021/acs.jced.9b00855.
[60] L. Neumaier, J. Schilling, A. Bardow, J. Gross, Dielectric constant of mixed solvents based on perturbation theory, Fluid Phase Equilib. 555 (2022), https://doi.org/10.1016/j.fluid.2021.113346.
[61] M. Bülow, M. Ascani, C. Held, ePC-SAFT advanced-Part I: Physical meaning of including a concentration-dependent dielectric constant in the born term and in the Debye-Hückel theory, Fluid Phase Equilib. 535 (2021).
[62] M. Bülow, M. Ascani, C. Held, ePC-SAFT advanced–Part II: Application to Salt Solubility in Ionic and Organic Solvents and the Impact of Ion Pairing, Fluid Phase Equilib. 537 (2021).
[63] S. Kournopoulos, A.J. Haslam, G. Jackson, A. Galindo, M. Schoen, Molecular theory of the static dielectric constant of dipolar fluids, J. Chem. Phys. 156 (2022), https://doi.org/10.1063/5.0079511.
[64] P.J. Walker, X. Liang, G.M. Kontogeorgis, Importance of the Relative Static Permittivity in electrolyte SAFT-VR Mie Equations of State, Fluid Phase Equilib. 551 (2022), https://doi.org/10.1016/j.fluid.2021.113256.
[65] N. Novak, G.M. Kontogeorgis, M. Castier, I.G. Economou, Modeling of Gas Solubility in Aqueous Electrolyte Solutions with the eSAFT-VR Mie Equation of State, Ind. Eng. Chem. Res. 60 (2021) 15327–15342, https://doi.org/10.1021/acs.iecr.1c02923.
[66] J.S. Roa Pinto, N. Ferrando, J.C. de Hemptinne, A. Galindo, Temperature dependence and short-range electrolytic interactions within the e-PPC-SAFT framework, Fluid Phase Equilib. 560 (2022), https://doi.org/10.1016/j.fluid.2022.113486.
[67] P. Debye, E. Huckel, Zur theorie der elektrolyte. i. gefrierpunktserniedrigung und verwandte erscheinungen, Phys. Z. 24 (1923) 185–206.
[68] D. Fraenkel, Simplified electrostatic model for the thermodynamic excess potentials of binary strong electrolyte solutions with size-dissimilar ions, Mol. Phys. 108 (11) (2010) 1435–1466.
[69] D. Fraenkel, Effect of solvent permittivity on the thermodynamic behavior of HCl solutions: Analysis using the smaller-ion shell model of strong electrolytes, J. Phys. Chem. B 115 (2011) 14634–14647.
[70] D. Fraenkel, Theoretical analysis of aqueous solutions of mixed strong electrolytes by a smaller-ion shell electrostatic model, J. Chem. Phys. 140 (2014) 54513.
[71] D. Fraenkel, Computing excess functions of ionic solutions: The smaller-ion shell model versus the primitive model. 1. Activity coefficients, J. Chem. Theory Comput. 11 (2015) 178–192, https://doi.org/10.1021/ct5006938.

[72] D. Fraenkel, Computing Excess Functions of Ionic Solutions: The Smaller-Ion Shell Model versus the Primitive Model. 2. Ion-Size Parameters, J. Chem. Theory Comput. 11 (2015) 193–204, https://doi.org/10.1021/ct500694u.
[73] J.-L. Liu, B. Eisenberg, Poisson-Fermi model of single ion activities in aqueous solutions, Chem. Phys. Lett. 637 (2015) 1–6.
[74] J.-L. Liu, C.-L. Li, A generalized Debye-Hückel theory of electrolyte solutions, AIP Adv. 9 (2019) 15214.
[75] C.-L. Li, J.-L. Liu, Generalized Debye-Hückel Equation From Poisson-Bikerman Theory, SIAM J. Appl. Math. 80 (5) (2020) 2003–2023.
[76] J.-L. Liu, B. Eisenberg, Molecular Mean-Field Theory of Ionic Solutions: A Poisson-Nernst-Planck-Bikerman Model, Entropy 22 (2020) 550, https://doi.org/10.3390/e22050550.
[77] C.-L. Li, S.-Y. Chou, J.-L. Liu, Generalized Debye-Hückel model for activity coefficients of electrolytes in water–methanol mixtures, Fluid Phase Equilib. 565 (2023), https://doi.org/10.1016/J.FLUID.2022.113662.
[78] I.Y. Shilov, A.K. Lyashchenko, The role of concentration dependent static permittivity of electrolyte solutions in the Debye-Huckel theory, J. Phys. Chem. B 119 (2015) 10087–10095.
[79] M. Valiskó, D. Boda, Comment on "The Role of Concentration Dependent Static Permittivity of Electrolyte Solutions in the Debye-Hückel Theory", J. Phys. Chem. B 119 (2015) 14332–14336, https://doi.org/10.1021/acs.jpcb.5b07750.
[80] I.Y. Shilov, A.K. Lyashchenko, Comment on "Predicting activity coefficients with the Debye-Hückel theory using concentration dependent static permittivity", AIChE J 68 (2022) e17515.
[81] A. González de Castilla, S. Müller, I. Smirnova, On the analogy between the restricted primitive model and capacitor circuits: Semi-empirical alternatives for over- and underscreening in the calculation of mean ionic activity coefficients, J. Mol. Liq. 326 (2021) 1–12, https://doi.org/10.1016/j.molliq.2020.115204.
[82] A. González de Castilla, S. Müller, I. Smirnova, On the analogy between the restricted primitive model and capacitor circuits. Part II: A generalized Gibbs-Duhem consistent extension of the Pitzer-Debye-Hückel term with corrections for low and variable relative permittivity, J. Mol. Liq. 360 (2022), https://doi.org/10.1016/j.molliq.2022.119398.
[83] G.M. Silva, X. Liang, G.M. Kontogeorgis, On the derivations of the Debye-Hückel equations, Mol. Phys. 120 (2022), https://doi.org/10.1080/00268976.2022.2064353.
[84] G.M. Silva, X. Liang, G.M. Kontogeorgis, Investigation of the Limits of the Linearized Poisson-Boltzmann Equation, J. Phys. Chem. B 126 (2022) 4112–4131, https://doi.org/10.1021/acs.jpcb.2c02758.
[85] G.M. Silva, X. Liang, G.M. Kontogeorgis, How to account for the concentration dependency of relative permittivity in the Debye-Hückel and Born equations, Fluid Phase Equilib. 566 (2023), https://doi.org/10.1016/J.FLUID.2022.113671.
[86] R. Kjellander, A multiple decay-length extension of the Debye-Hückel theory: To achieve high accuracy also for concentrated solutions and explain underscreening in dilute symmetric electrolytes, PCCP 22 (2020) 23952–23985, https://doi.org/10.1039/d0cp02742a.
[87] J.-S. Jon, W.-K. Ri, K.-R. Sin, Y.-C. Son, K.-W. Jo, J.-S. Pak, S.-J. Kim, Y.-J. Ri, Y.-C. An, Derivation of the solvation effect-incorporated Poisson-Boltzmann equation, J. Mol. Liq. 351 (2022), https://doi.org/10.1016/j.molliq.2022.118537.
[88] M. Born, Volumen und Hydratationswärme der Ionen, Z. Phys. 1 (1920) 45–48, https://doi.org/10.1007/BF01881023.
[89] I.Y. Shilov, A.K. Lyashchenko, Modeling activity coefficients in alkali iodide aqueous solutions using the extended Debye-Hückel theory, J. Mol. Liq. 240 (2017) 172–178.
[90] Q. Lei, B. Peng, L. Sun, J. Luo, Y. Chen, G.M. Kontogeorgis, X. Liang, Predicting activity coefficients with the Debye-Hückel theory using concentration dependent static permittivity, AIChE J 66 (2020) e16651.
[91] L. Sun, Q. Lei, B. Peng, G.M. Kontogeorgis, X. Liang, An analysis of the parameters in the Debye-Hückel theory, Fluid Phase Equilib. 556 (2022), https://doi.org/10.1016/j.fluid.2022.113398.
[92] S. Naseri Boroujeni, X. Liang, B. Maribo-Mogensen, G.M. Kontogeorgis, Comparison of Models for the Prediction of the Electrical Conductivity of Electrolyte Solutions, Ind. Eng. Chem. Res. 61 (2022) 3168–3185, https://doi.org/10.1021/acs.iecr.1c04365.
[93] X. Liang, M.L. Michelsen, G.M. Kontogeorgis, Pitfalls of using the geometric-mean combining rule in the density gradient theory, Fluid Phase Equilib. 415 (2016) 75–83, https://doi.org/10.1016/j.fluid.2016.01.047.
[94] X. Liang, M.L. Michelsen, General approach for solving the density gradient theory in the interfacial tension calculations, Fluid Phase Equilib. 451 (2017), https://doi.org/10.1016/j.fluid.2017.07.021.
[95] E.L. Camacho Vergara, G.M. Kontogeorgis, X. Liang, Gas Adsorption and Interfacial Tension with Classical Density Functional Theory, Ind. Eng. Chem. Res. 58 (2019) 5650–5664, https://doi.org/10.1021/acs.iecr.9b00137.
[96] J. Mairhofer, J. Gross, Modeling properties of the one-dimensional vapor-liquid interface: Application of classical density functional and density gradient theory, Fluid Phase Equilib. 458 (2018) 243–252, https://doi.org/10.1016/j.fluid.2017.11.032.
[97] P. Rehner, J. Gross, Predictive density gradient theory based on nonlocal density functional theory, Phys. Rev. E 98 (2018) 63312, https://doi.org/10.1103/PhysRevE.98.063312.
[98] J. Gross, G. Sadowski, Application of perturbation theory to a hard-chain reference fluid: an equation of state for square-well chains, Fluid Phase Equilib. 168 (2000) 183–199, https://doi.org/10.1016/S0378-3812(00)00302-2.
[99] T. Lafitte, A. Apostolakou, C. Avendaño, A. Galindo, C.S. Adjiman, E.A. Müller, G. Jackson, Accurate statistical associating fluid theory for chain molecules formed from Mie segments, J. Chem. Phys. 139 (2013), https://doi.org/10.1063/1.4819786.
[100] A.P. Thompson, H.M. Aktulga, R. Berger, D.S. Bolintineanu, W.M. Brown, P.S. Crozier, P.J. in 't Veld, A. Kohlmeyer, S.G. Moore, T.D. Nguyen, R. Shan, M.J. Stevens, J. Tranchida, C. Trott, S.J. Plimpton, LAMMPS - a flexible simulation tool for particle-based materials modeling at the atomic, meso, and continuum scales, Comput. Phys. Commun. 271 (2022) 108171.
[101] J.M. Martínez, L. Martínez, Packing optimization for automated generation of complex system's initial configurations for molecular dynamics and docking, J. Comput. Chem. 24 (2003) 819–825, https://doi.org/10.1002/jcc.10216.
[102] L. Martínez, R. Andrade, E.G. Birgin, J.M. Martínez, PACKMOL: A package for building initial configurations for molecular dynamics simulations, J. Comput. Chem. 30 (2009) 2157–2164, https://doi.org/10.1002/jcc.21224.
[103] A.I. Jewett, D. Stelter, J. Lambert, S.M. Saladi, O.M. Roscioni, M. Ricci, L. Autin, M. Maritan, S.M. Bashusqeh, T. Keyes, R.T. Dame, J.E. Shea, G.J. Jensen, D.S. Goodsell, Moltemplate: A Tool for Coarse-Grained Modeling of Complex Biological Matter and Soft Condensed Matter Physics, J. Mol. Biol. 433 (2021), https://doi.org/10.1016/j.jmb.2021.166841.
[104] J. Vincze, M. Valiskó, D. Boda, The nonmonotonic concentration dependence of the mean activity coefficient of electrolytes is a result of a balance between solvation and ion-ion correlations, J. Chem. Phys. 133 (2010), https://doi.org/10.1063/1.3489418.
[105] M. Valiskó, D. Boda, Unraveling the behavior of the individual ionic activity coefficients on the basis of the balance of ion-ion and ion-water interactions, J. Phys. Chem. B 119 (2015) 1546–1557, https://doi.org/10.1021/jp509445k.
[106] B. Maribo-Mogensen, G.M. Kontogeorgis, K. Thomsen, Modeling of Dielectric Properties of Complex Fluids with an Equation of State, J. Phys. Chem. B 117 (2013) 3389–3397, https://doi.org/10.1021/jp310572q.
[107] B. Maribo-Mogensen, G.M. Kontogeorgis, K. Thomsen, Modeling of dielectric properties of aqueous salt solutions with an equation of state, J. Phys. Chem. B 117 (36) (2013) 10523–10533.
[108] H.-L. Zhang, S.-J. Han, Viscosity and Density of Water + Sodium Chloride + Potassium Chloride Solutions at 298.15 K, J. Chem. Eng. Data 41 (1996) 516–520.
[109] P. Novotny, O. Sohnel, Densities of binary aqueous solutions of 306 inorganic substances, J. Chem. Eng. Data 33 (1) (1988) 49–55.
[110] M.P. Allen, D.J. Tildesley, Computer Simulation of Liquids: Second Edition, 2nd ed., Oxford University Press, Oxford, 2017. 10.1093/oso/9780198803195.001.0001.
[111] C. Cadena, Q. Zhao, R.Q. Snurr, E.J. Maginn, Molecular Modeling and Experimental Studies of the Thermodynamic and Transport Properties of Pyridinium-Based Ionic Liquids, J. Phys. Chem. B 110 (2006) 2821–2832, https://doi.org/10.1021/jp056235k.
[112] Z. Liu, T. Chen, A. Bell, B. Smit, Improved United-Atom Force Field for 1-Alkyl-3-methylimidazolium Chloride, J. Phys. Chem. B 114 (2010) 4572–4582, https://doi.org/10.1021/jp911337f.
[113] E.J. Maginn, R.A. Messerly, D.J. Carlson, D.R. Roe, J.R. Elliot, Best Practices for Computing Transport Properties 1. Self-Diffusivity and Viscosity from Equilibrium Molecular Dynamics [Article v1.0], Living J Comput Mol Sci. 1 (2018) 6324.
[114] S.H. Lee, Ionic mobilities of Na+ and Cl− at 25°C as a function of Ewald sum parameter: a comparative molecular dynamics simulation study, Mol. Simul. 46 (2020) 262–270, https://doi.org/10.1080/08927022.2019.1696966.
[115] S.H. Lee, Dynamic and Static Properties of Aqueous NaCl Solutions at 25°C as a Function of NaCl Concentration: A Molecular Dynamics Simulation Study, J. Chem. 2020 (2020), https://doi.org/10.1155/2020/6661196.
[116] R. Mills, A.W. Adamson, The Measurement of Self-diffusion in Electrolyte Solutions, J. Am. Chem. Soc. 77 (1955) 3454–3458, https://doi.org/10.1021/ja01618a007.
[117] R. Mills, A Remeasurement of the Self-diffusion Coefficients of Sodium Ion in Aqueous Sodium Chloride Solutions, J. Am. Chem. Soc. 77 (1955) 6116–6119, https://doi.org/10.1021/ja01628a008.
[118] R. Mills, The self-diffusion of chloride ion in aqueous alkali chloride solutions at 25°, J. Phys. Chem. 61 (1957) 1631–1634, https://doi.org/10.1021/j150558a015.
[119] R. Mills, E.W. Godbole, VERIFICATION OF THE ONSAGER LIMITING LAW FOR TRACE-ION DIFFUSION IN ELECTROLYTE SOLUTIONS, J. Am. Chem. Soc. 82 (1960) 2395–2396, https://doi.org/10.1021/ja01494a071.
[120] P. Passiniemi, Accurate tracer diffusion coefficients of Na+ and Cl- ions in dilute aqueous sodium chloride solutions measured with the closed capillary method, J. Solution Chem. 12 (1983) 801–813, https://doi.org/10.1007/BF00653183.
[121] K.R. Harris, R. Mills, P.J. Back, D.S. Webster, An improved NMR spin-echo apparatus for the measurement of self-diffusion coefficients: The diffusion of water in aqueous electrolyte solutions, J. Magn. Reson. 29 (1978) (1969) 473–482, https://doi.org/10.1016/0022-2364(78)90005-7.
[122] I.C. Yeh, G. Hummer, System-size dependence of diffusion coefficients and viscosities from molecular dynamics simulations with periodic boundary

conditions, J. Phys. Chem. B 108 (2004) 15873–15879, https://doi.org/10.1021/jp0477147.
[123] H.G. Hertz, Velocity Correlations in Aqueous Electrolyte Solutions from Diffusion, Conductance, and Transference Data. Part 1, Theory, Ber. Bunsen. Phys. Chem 81 (7) (1977) 656–664.
[124] H.G. Hertz, K.R. Harris, R. Mills, L.A. Woolf, Velocity Correlations in Aqueous Electrolyte Solutions from Diffusion, Conductance, and Transference Data. Part 2, Applications to Concentrated Solutions of 1–1 Electrolytes, Berichte Der Bunsengesellschaft Für Physikalische, Chemie. 81 (1977) 664–670, https://doi.org/10.1002/bbpc.19770810708.
[125] L.A. Woolf, K.R. Harris, Velocity correlation coefficients as an expression of particle–particle interactions in (electrolyte) solutions, Journal of the Chemical Society, Faraday Transactions 1: Physical Chemistry in Condensed Phases. 74 (1978) 933–947. 10.1039/F19787400933.
[126] K.R. Harris, H.J.V. Tyrrell, Hartley–Crank equation and standard velocity correlation coefficients, Journal of the Chemical Society, Faraday Transactions 1: Physical Chemistry in Condensed Phases. 78 (1982) 957–960. 10.1039/F19827800957.
[127] K.R. Harris, Comment on "ionic Conductivity, Diffusion Coefficients, and Degree of Dissociation in Lithium Electrolytes, Ionic Liquids, and Hydrogel Polyelectrolytes", J. Phys. Chem. B 122 (2018) 10964–10967, https://doi.org/10.1021/acs.jpcb.8b08610.
[128] L.A. Woolf, K.R. Harris, S.A. Fairhurst, L.H. Sutcliffe, Corrigenda, Journal of the Chemical Society, Faraday Transactions 1: Physical Chemistry in Condensed Phases. 75 (1979) 2873. 10.1039/F19797502873.
[129] W.C. Bray, F.L. Hunt, THE CONDUCTANCE OF AQUEOUS SOLUTIONS OF SODIUM CHLORIDE, HYDROCHLORIC ACID AND THEIR MIXTURES, J. Am. Chem. Soc. 33 (1911) 781–795, https://doi.org/10.1021/ja02219a002.
[130] T. Shedlovsky, AN EQUATION FOR ELECTROLYTIC CONDUCTANCE, J. Am. Chem. Soc. 54 (1932) 1405–1411, https://doi.org/10.1021/ja01343a019.
[131] P. van Rysselberghe, S.W. Grinnell, J.M. Carlson, Conductivities of Concentrated Binary Mixtures of Electrolytes with a Common Anion and at Least One Ion of Charge Two, J. Am. Chem. Soc. 59 (1937) 336–339, https://doi.org/10.1021/ja01281a034.
[132] R.W. Bremner, T.G. Thompson, C.L. Utterback, Electrical Conductances of Pure and Mixed Salt Solutions in the Temperature Range 0 to 25°, J. Am. Chem. Soc. 61 (1939) 1219–1223, https://doi.org/10.1021/ja01874a060.
[133] H.E. Gunning, A.R. Gordon, The Conductance and Ionic Mobilities for Aqueous Solutions of Potassium and Sodium Chloride at Temperatures from 15° to 45°C, J. Chem. Phys. 10 (1942) 126–131, https://doi.org/10.1063/1.1723667.
[134] G.C. Benson, A.R. Gordon, The Conductance of Aqueous Solutions of Calcium Chloride at Temperatures from 15° to 45°C, J. Chem. Phys. 13 (1945) 470–472, https://doi.org/10.1063/1.1723980.
[135] G.C. Benson, A.R. Gordon, A Reinvestigation of the Conductance of Aqueous Solutions of Potassium Chloride, Sodium Chloride, and Potassium Bromide at Temperatures from 15° to 45°C, J. Chem. Phys. 13 (1945) 473–474, https://doi.org/10.1063/1.1723981.
[136] J.F. Chambers, J.M. Stokes, R.H. Stokes, Conductances of concentrated aqueous sodium and potassium chloride solutions at 25°, J. Phys. Chem. 60 (1956) 985–986, https://doi.org/10.1021/j150541a040.
[137] R. Holze, Ionic conductance of NaCl: Datasheet from Physical Chemistry · Volume 9B2: "Electrochemistry" in SpringerMaterials (https://doi.org/10.1007/978-3-662-49251-2_1338), (n.d.). 10.1007/978-3-662-49251-2_1338.
[138] A. Ghaffari, A. Rahbar-Kelishami, MD simulation and evaluation of the self-diffusion coefficients in aqueous NaCl solutions at different temperatures and concentrations, J. Mol. Liq. 187 (2013) 238–245, https://doi.org/10.1016/j.molliq.2013.08.004.
[139] W.R. Fawcett, Thermodynamic Parameters for the Solvation of Monatomic Ions in Water, J. Phys. Chem. B 103 (1999) 11181–11185, https://doi.org/10.1021/jp991802n.
[140] R. Schmid, A.M. Miah, V.N. Sapunov, A new table of the thermodynamic quantities of ionic hydration: values and some applications (enthalpy–entropy compensation and Born radii), PCCP 2 (2000) 97–102, https://doi.org/10.1039/A907160A.
[141] G. Hummer, L.R. Pratt, A.E. García, Free Energy of Ionic Hydration, J. Phys. Chem. 100 (1996) 1206–1215, https://doi.org/10.1021/jp951011v.
[142] Y. Marcus, A simple empirical model describing the thermodynamics of hydration of ions of widely varying charges, sizes, and shapes, Biophys. Chem. 51 (1994) 111–127, https://doi.org/10.1016/0301-4622(94)00051-4.
[143] R. Buchner, G.T. Hefter, P.M. May, Dielectric Relaxation of Aqueous NaCl Solutions, Chem. A Eur. J. 103 (1999) 1–9, https://doi.org/10.1021/jp982977k.
[144] V.V. Shcherbakov, Y.M. Artemkina, E.N. Korotkova, Dielectric properties and high-frequency conductivity of the sodium chloride-water system, Russ. J. Inorg. Chem. 59 (9) (2014) 922–926.
[145] M. Valiskó, D. Boda, The effect of concentration- and temperature-dependent dielectric constant on the activity coefficient of NaCl electrolyte solutions, J. Chem. Phys. 140 (2014), https://doi.org/10.1063/1.4883742.
[146] CERE DTU, DTU Electrolyte Database, CERE DTU. (n.d.). https://www.cere.dtu.dk/Expertise/Data-for-aqueous-salt-solutions (accessed August 27, 2021).
[147] F. Yang, T. Dat Ngo, G.M. Kontogeorgis, J.-C. de Hemptinne, A Benchmark Database for Mixed-Solvent Electrolyte Solutions: Consistency Analysis Using E-NRTL, Ind. Eng. Chem. Res. 61 (2022) 15576–15593, https://doi.org/10.1021/acs.iecr.2c00059.
[148] J.V. Sengers, B. Kamgar-Parsi, Representative Equations for the Viscosity of Water Substance, J. Phys. Chem. Ref. Data 13 (1) (1984) 185–205.